

Supporting Information

The effects of surface charge on intra-tumor penetration of drug delivery vehicles along with tumor progression

Donglin Han^a, Hongzhao Qi^{a,c}, Kai Huang^b, Xueping Li^a, Qi Zhan^a, Jin Zhao^a, Xin Hou^a, Xianjin Yang^a, Chunsheng Kang^{b,*}, Xubo Yuan^{a,*}

Supporting figures for results and discussion

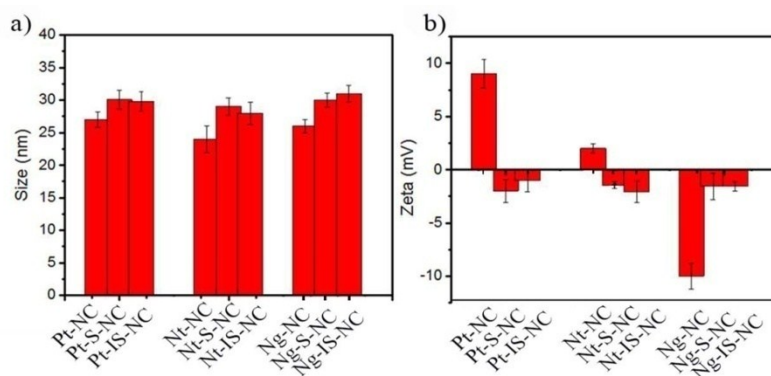


Figure S1. Characterization of pH-not-responsive nanocapsules. a) DLS measuring the size. b) the surface zeta potential.

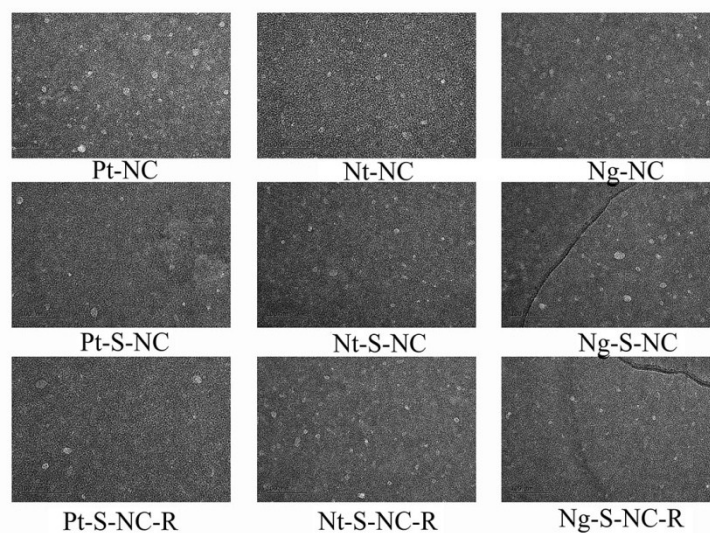


Figure S2. TEM showing the morphology of nanocapsules before and after modification of PGE

shell.

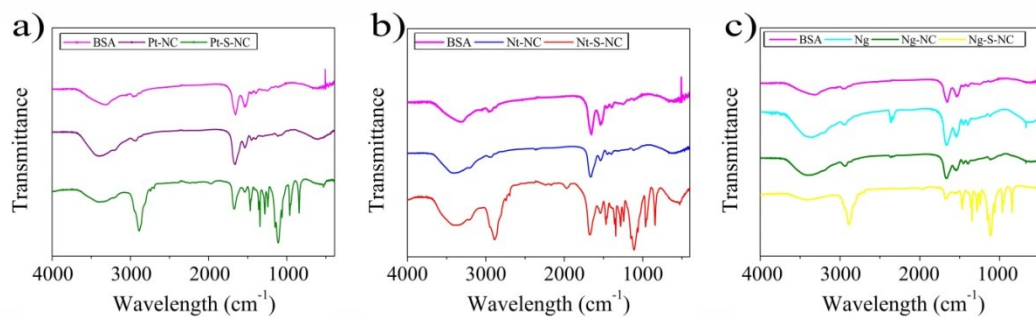


Figure S3. The infrared spectra of nanocapsules. a) nanocapsules with positive surface charge. b) nanocapsules with neutral surface charge. c) nanocapsules with negative surface charge.

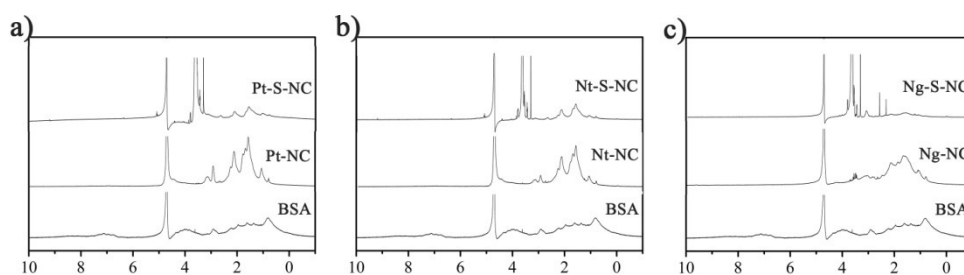


Figure S4. The ^1H NMR spectra of nanocapsules in D_2O . a) nanocapsules with positive surface charge. b) nanocapsules with neutral surface charge. c) nanocapsules with negative surface charge.

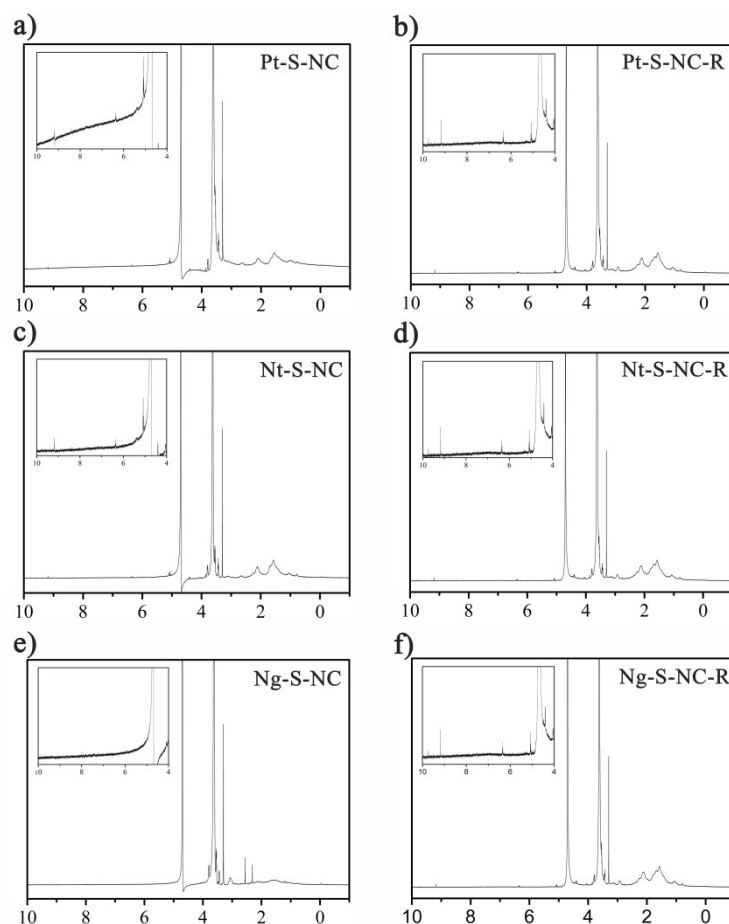


Figure S5. The ^1H NMR spectra of nanocapsules in D_2O . a,b) nanocapsules with positive surface charge. c,d) nanocapsules with neutral surface charge. e,f) nanocapsules with negative surface charge.

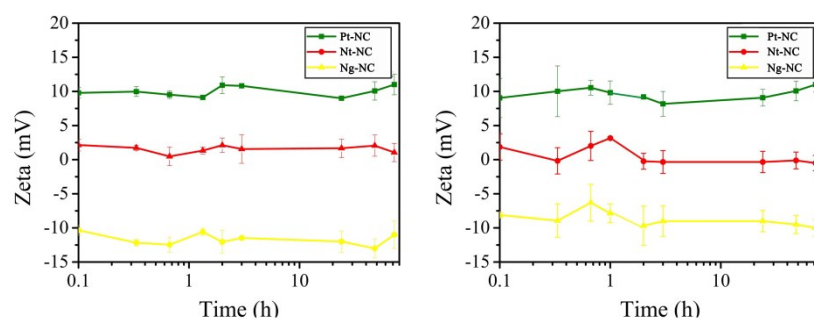


Figure S6. In vitro stability of nanocapsules with different surface charge in PB. a) pH=6.8.
b) pH=7.4.

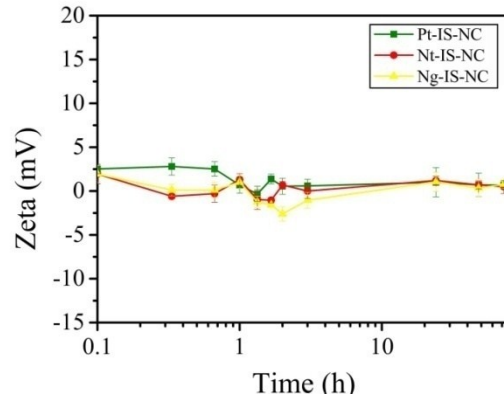


Figure S7. In vitro stability of pH-not-responsive nanocapsules in PB (pH=6,8).

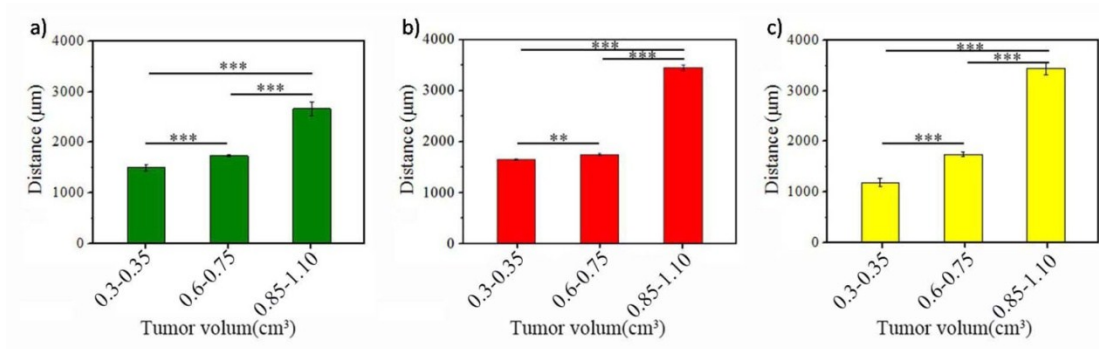


Figure S8. The penetrating ability of nanoparticles with the same surface zeta potential in tumors of different sizes. a) Pt-S-NC. b) Nt-S-NC. c) Ng-S-NC, (n=3, *p<0.05, **P<0.01, ***P,0.005).

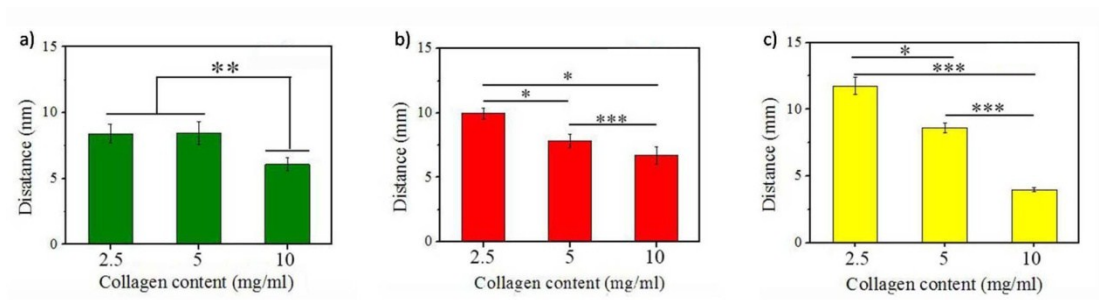


Figure S9. The penetration distance of nanocapsules in collagen hydrogel of different concentration. a) Pt-S-NC. b) Nt-S-NC. c) Ng-S-NC, (n=3, *p<0.05, **P<0.01, ***P<0.005).